A detailed paleomagnetic and rock-magnetic investigation around Cretaceous-Paleogene boundary: the Autlan (Western Mexico) volcanic sequence revisited

MIGUEL CERVANTES-SOLANO[1], LISA KAPPER[2], AVTO GOGUITCHAICHVILI[2], VICENTE CARLOS RUIZ-MARTÍNEZ[3], JOSÉ ROSAS-ELGUERA[4], JUAN MORALES[2], RAFAEL MACIEL-PEÑA[5] AND RUBÉN CEJUDO-RUIZ[2]

1 Laboratorio Interinstitucional de Magnetismo Natural, Sede Escuela Nacional de Estudios Superiores, Campus Morelia, Universidad Nacional Autónoma de México, 58190 Morelia, México (miguel_cervantes@enesmorelia.unam.mx)

2 Instituto de Geofisica, Unidad Michoacán, Universidad Nacional Autonoma de México, Campus Morelia, 58190 Morelia, México

3 Departamento de Geofísica, Facultad de Física, Universidad Complutense de Madrid, Spain

4 Laboratorio Interinstitucional de Magnetismo Natural, Sede Universidad de Guadalajara, México

5 Laboratorio Interinstitucional de Magnetismo Natural, Sede Instituto Tecnologico de Estudios Superiores Tacambaro, Michoacan, México

Received: April 19, 2016; Revised: July 7, 2016; Accepted: October 18, 2016

ABSTRACT

We present a detailed rock-magnetic and paleomagnetic survey from Autlan volcanic succession in western Mexico. The principal aim of this study is to extend paleomagnetic data from Autlan lavas in order to confirm vertical-axis rotation observed in reconnaissance study and to evaluate long-term variation of the geomagnetic field strength based on existing and global data. The mean inclination (44.7°) is in agreement with the expected inclination for 60 and 70 Ma, as derived from available reference poles for the North American craton. The declination (333.6°), however, is significantly different from those expected, which suggests a statistically significant counterclockwise tectonic rotation ranging between 10° ± 6° and 14° ± 7°. As a measure of paleosecular variation (PSV), we obtained a geomagnetic field dispersion of 9.6° (upper and lower limits: 7.2°–11.9°) in perfect agreement with the previously published PSV compilation of selected Cretaceous data from lavas. The mean virtual dipole moments available for Autlan lavas are about 65% of the present geomagnetic axial dipole but are in reasonably good agreement with other comparable quality determinations between 5 and 90 Ma. This reinforces the hypothesis that low geomagnetic field strengths persisted for the entire Jurassic extending into the Upper Cretaceous.

Keywords: Upper Cretaceous, paleomagnetism, Western Mexico, rock-magnetism, vertical axis rotation, magnetostratigraphy

1. INTRODUCTION

Secular variations and reversals of the main geomagnetic field components are now well constrained for the last 180 Ma. During the whole Paleogene–Neogene period, the Earth's magnetic field experienced multiple reversals and excursions while there is a long period of normal polarity (about 37 Myr) during the Cretaceous called as the Cretaceous Normal Superchron (*Opdyke and Channell, 1996*). *Tarduno and Smirnov (2001)* suggest that the time-averaged field during the Cretaceous Normal Polarity Superchron was unusually high and stable. Some evidences of high field were also reported by *Tauxe and Staudigel (2004)* from study of submarine basaltic glass. Thus, the Cretaceous should be definitively considered as a key period for the long-term evolution of the geomagnetic field. In other hand, systematic and high standard paleomagnetic surveys varied out on Cretaceous volcanic rocks may provide some decisive constraints on the existence of the Mesozoic Dipole Low (MDL) characterized by low absolute intensity (*Prevot et al., 1990*; *Tanaka et al., 1995*). However, the duration and even existence of the MDL is not estimated and understood (*Goguitchaichvili et al., 2002*; *Tarduno and Cotrell, 2005*; see also *Perrin and Shcherbakov, 1997*).

Most of paleomagnetic studies in Mexico is concentrated in the Trans-Mexican volcanic belt (TMVB) with contrasting results (*Goguitchaichvili et al., 2004*). Reliable Paleomagnetic data from the western and eastern TMVB as well as from sourrounding terrains are scarce which limits analyses of the regional geodynamic evolution. *Böhnel et al. (1989)* presented detailed paleomagnetic results for more than 100 sites in different intrusive, volcanic, and sedimentary units exposed along the southern Mexico continental margin (Guerrero Terrane). This study was aimed to estimate the accretion history of the Guerrero terrane and subsequent movements of the margin. The authors reported evidence of several tectonic rotations. Many sites showed low to moderate degree of metamorphism which makes difficult to retrieve the primary, characteristic remanent magnetization.

Cretaceous volcanic sequences from Western Mexico represent good target for systematic paleomagnetic survey. *Goguitchaichvili et al. (2003, 2004)* studied fifteen radiometrically dated (67.4 ± 1.2 Ma) lava flows at the Sierra Cacoma area (Jalisco block, Western Mexico). The mean paleodirection obtained from 14 sites pointed to a counterclockwise tectonic rotation for this region within the Jalisco block. The absolute paleointensity determination was also intended. 18 individual samples from four independent lava flows yielded a mean virtual dipole moment of $4.9 \pm 0.6 \times 10^{22}$ Am^2, which is significantly lower than the present geomagnetic field strength. However, both geodynamic and geomagnetic outcomes are based on a limited number of samples and thus no firm conclusions may be achieved. In the present study we sampled twelve additional lava flows from the same area (located at 19.7°N, 104.4°W) in order to obtain a robust paleomagnetic dataset for the Upper Cretaceous. The principal aim of this study is to extend paleomagnetic data from Autlan lavas in order to confirm vertical-axis rotation observed in reconnaissance study and to evaluate long-term variation of the geomagnetic field strength based on existing and global data.

2. GEOLOGICAL CONTEXT AND SAMPLING

The study area belongs to the Guerrero terrane (Fig. 1a), formed of sedimentary, volcano-sedimentary and volcanic rocks (*Campa and Coney, 1983*), and represents a main period of magmatism during Mesozoic. The Jalisco block, a fault bounded crustal block belonging to the Guerrero terrane, includes intrusive rocks of the Puerto Vallarta batholith

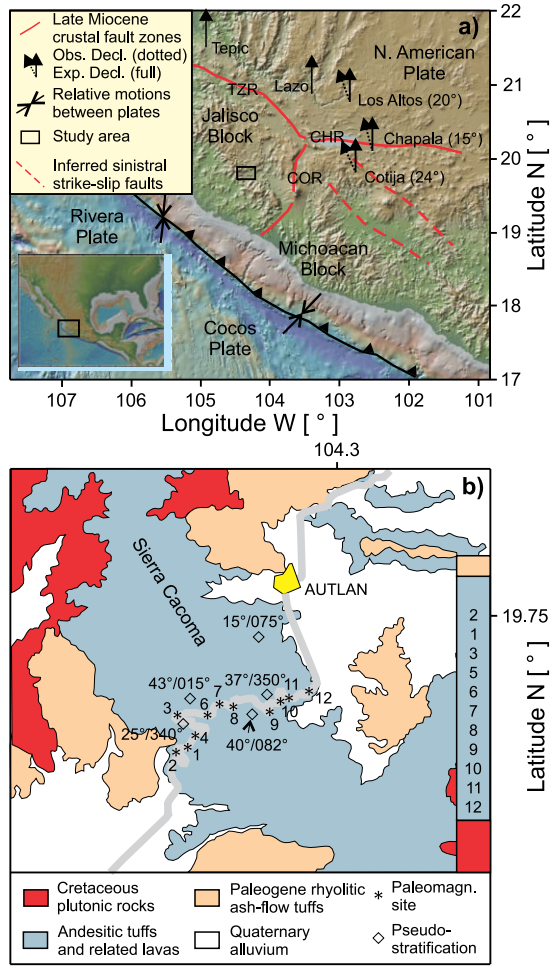

Fig. 1. **a)** Tectonic framework for the Jalisco block. Extensional deformation along the continental boundaries are related to a normal (Rivera Plate) and oblique (Cocos Plate) convergence relative to the continental blocks. Note that volcanic fields inside the Jalisco block are not affected by faulting. TZR: Tepic-Zacoalco Rift, COR: Colima Rift, CHR: Chapala Rift. **b)** A simplified geologic map of Autlan area with indication of paleomagnetic sites; the dip and strike reported refers to the apparent flow directions. The simplified stratigraphic column on the right shows approximate stratigraphic position of the samples. After Servicio Geologico Mexicano, 1997.

with ages ranging between 133 and 61 Ma (*Valencia et al., 2013*, and references therein), which belong to a plutonic belt parallel to the present-day Middle America Trench. The schists sampled along the boundaries of the intrusive rocks gave ages between 135 and 161 Ma (*Valencia et al., 2013*).

Valencia et al (2013) define the Carmichael silicic ash flow tuff volcanic succession which comprises a widespread silicic ash flow tuffs, volcanic breccias, lithic tuffs, ad tuff breccias with ages ranging between 58 and 83 Ma. North of the Autlan area a silicic ash flow tuff overlying an andesitic succession of volcanic breccias and lithic tuffs gave 66.8 Ma (*Valencia et al., 2013*). To the east of Autlan we studied a succession of andesitic volcanic breccias up to 300 m thick (Fig. 1a) where a mafic unit is characterized by large feldspar crystals (up to 2 cm) appears at the base of this succession. This succession is overlying by a flat-lying rhyolitic ash-flow tuff dated in 66.8 Ma by *Valencia et al. (2013)* and belongs to Carmichael´s volcanic succession.

119 oriented samples belonging to 12 volcanic units were collected at fresh road-cuts southwest of Autlan city (Fig. 1b), in flows interspersed among those previously studied by *Goguitchaichvili et al. (2003)*. The whole-rock sample from the middle part of sequence yielded a K-Ar age of 67.4 ± 1.2 Ma (1.99%K, 85.8% ^{40}Ar*) (*Goguitchaichvili et al., 2003*). Commonly, the outcrops extend laterally over a few tens of meters, and in these cases we drilled typically 8–12 standard paleomagnetic cores per site. The samples were distributed throughout each flow both horizontally and vertically in order to minimize effects of block tilting and lightning. Cores were obtained with a gasoline-powered portable drill, and then oriented with both magnetic and sun compasses. Some lava flows sampled are sub-horizontal, while others present well-defined planes which are considered as 'original' tilting occurred during the emplacement. The dip and strike measurements shown on simplified geological map refers to the bedding plane of lava planes. Thus, no tectonic correction was applied in this study.

3. METHODS

In order to characterize in more detail the magnetic remanence carriers and their domain state a set of rock-magnetic experiments was undertaken. With the aid of a Variable Field Translation Balance (MM_VFTB), we performed progressive isothermal remanent magnetization (*IRM*) acquisition curves, hysteresis loops (±1 T), backfield coercivity curves and thermomagnetic (Fig. 2) curves (magnetization vs. temperature) up to 700°C in air. These analyses were carried out on bulk sample (~450 mg) per lava flow. Hysteresis and backfield data were treated by using the the RockMagAnalyzer 1.0 software (*Leonhardt, 2006*). The saturation magnetization (M_s), remanent saturation magnetization (M_{rs}), and coercive field (B_c) were calculated from hysteresis loops after subtracting the paramagnetic contribution. These parameters combined with the coercivity of remanence (B_{cr}), obtained independently from the backfield curves, allowed us to estimate the domain state distribution of the collection in the Day plot (*Day et al., 1977*; *Dunlop, 2002*). The Curie temperatures of themomagnetic curves were determined with the two-tangent method of *Grommé et al. (1969)*.

In order to isolate the characteristic remanent magnetization (*ChRM*), the stepwise progressive demagnetization of the natural remanent magnetization (*NRM*) by alternating

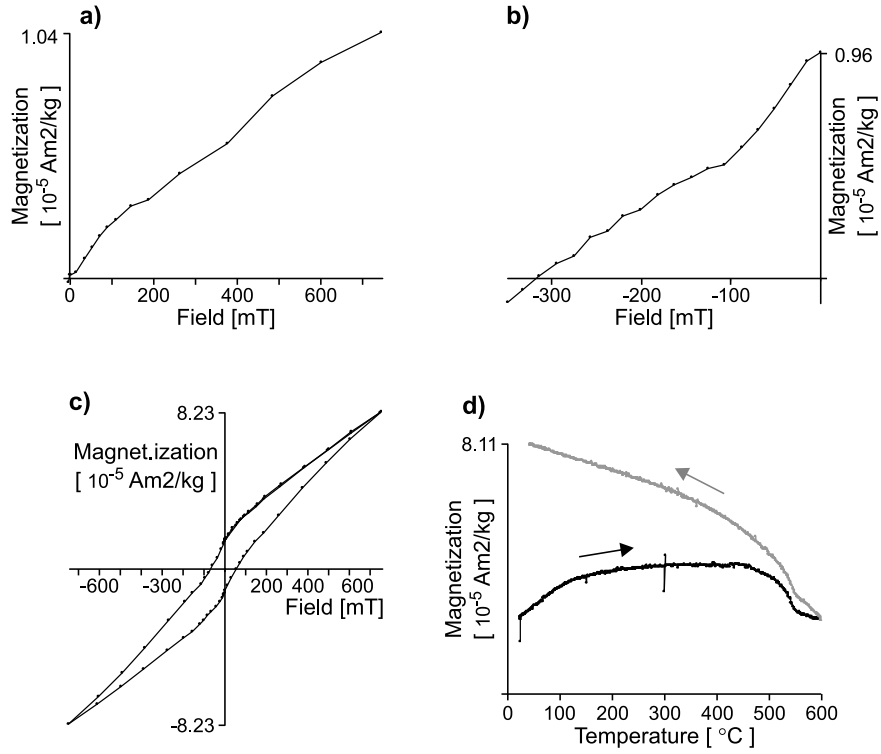

Fig. 2. Examples of rock-magnetic results, Sample BJ-093: **a)** isothermal remanent acquisition curve, **b)** back-field curve to determine the coercivity of remanence, **c)** hysteresis loop, and **d)** continuous thermomagnetic curve.

field (AF) or thermal (TH) demagnetization was applied. AF demagnetization (Fig. 3) was carried out in 5 to 9 steps up to a maximum peak field of 90 mT using Molspin demagnetizer. Thermal demagnetization was performed up to 565°C using a TD48-SC (ASC) thermal demagnetizer. A JR6a AGICO spinner magnetometer was used to measure remanence vectors of the initial *NRM* and after each demagnetization step. The *ChRM* direction for each sample was calculated by the method of the principal component analysis (*Kirschvink, 1980*), involving a minimum of 5 demagnetization steps including the origin. Mean directions and associated statistical parameters were calculated using *Fisher (1953)* statistics (95% confidence limit α_{95}, precision parameter k).

The Thellier-Coe type experiments (*Thellier and Thellier, 1959*; *Coe, 1967*) were carried out using an ASC ScientificTD48-SC furnace; all heating/cooling runs were performed in air. The laboratory field strength was set to 40 μT. Partial thermoremanent magnetization reinvestigations (*pTRM* checks) at each third temperature steps were added to the protocol.

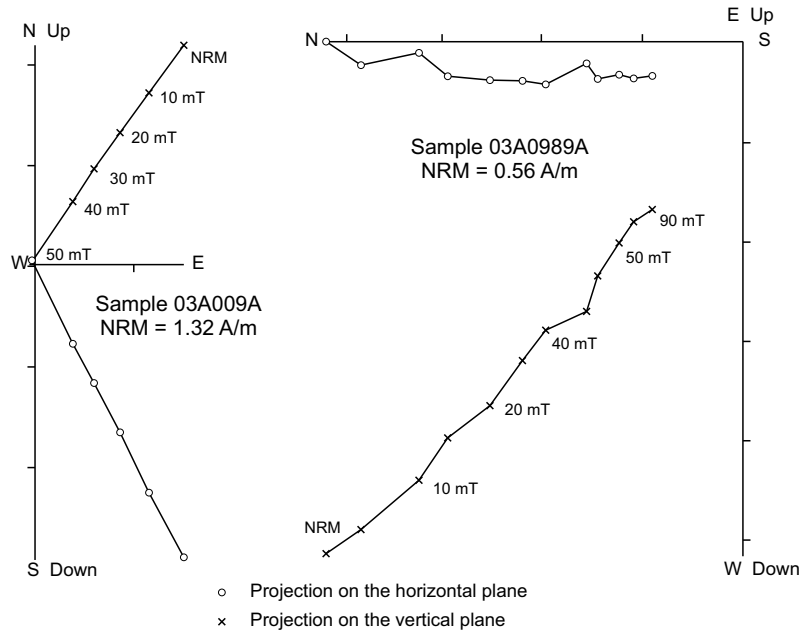

Fig. 3. Orthogonal vector plots of stepwise alternating field demagnetization (stratigraphic coordinates). The numbers refer to peak alternating field.

4. RESULTS AND DISCUSSION

As rock-magnetic properties are concerned it appears that the majority of progressive *IRM* acquisition curves are almost saturated between 130–250 mT, indicating that the remanent magnetization is dominated by low-coercivity minerals (titanomagnetite or titanomaghemite). However, some (few) samples do not reach complete saturation upon maximum available fields applied, pointing out that a considerable fraction of high-coercivity is also present (sample BJ-093, Fig. 2a). This sample is characterized with high remanence coercivity (Fig. 2b) and apparently wasp-waisted hysteresis loop (Fig. 2c). All these factors may indicate the co-existence of (titano)magnetite and (titano)hematite as main magnetic carriers. The thermomagnetic curve reinforces this hypothesis as two magnetic phases are detectable during the heating being the second phase compatible to almost pure hematite.

Figure 3 illustrates representative examples of *NRM* orthogonal demagnetization diagrams. The *NRM* (natural remanent magnetization) stability in AF samples is defined by a stable single component which is almost completely demagnetized at 50 mT (Fig. 3, sample 03A009A), indicating that the dominant *NRM* carrier is a low-coercivity mineral. There are very few exceptions, as the sample 03A098A shown in Fig. 3 with almost 20% of the initial *NRM* remaining at 90 mT due to the contribution of a high-coercivity mineral, most probably haematite. In any case, the *ChRM* direction can be successfully isolated here.

Table 1. Site-mean remanence paleodirections for Autlan volcanics. *n*: number of specimens used for calculation (in italics are sites with $n < 5$); *N*: number of treated samples; *Inc*: inclination; *Dec*: declination (reversed site-mean directions marked in bold type); α_{95} and *k*: radius of 95% confidence angle and precision parameter of *Fisher (1953)* statistics; *Plat* and *Plong*: paleolatitude and paleolongitude of virtual geomagnetic poles, respectively (all in northern hemisphere coordinates). BJ: this study; AU: *Goguitchaichvili et al. (2003)*; N.D.: not determined. Data in bold are the sites with reversed polarity.

Site	*n*	*N*	*Inc* [°]	*Dec* [°]	α_{95} [°]	*k*	*Plat* [°]	*Plong* [°]
BJ12	5	8	56.7	10.8	8.8	62	70.1	–78.4
BJ11	8	8	52.3	343.8	6.7	86	70.4	–148.7
BJ10	6	7	34.4	330.3	9.6	52	62.0	–191.0
BJ9	6	8	48.3	331.4	7.5	79	62.3	–168.5
BJ8	8	8	53.4	337.6	8.3	68	65.5	–154.2
BJ7	5	8	48.2	324.1	7.8	96	56.1	–171.1
BJ6	*0*	*8*	*N.D.*	*N.D.*	*N.D.*	*N.D.*	*N.D.*	*N.D.*
BJ5	5	7	53.7	320.5	6.3	156	52.2	–163.5
BJ3	6	8	43.2	321.6	7.1	117	54.4	–178.5
BJ4	*4*	*6*	*40.6*	*317.8*	*11.6*	*42*	*50.7*	*–181.5*
BJ1	8	8	**–25.8**	**163.1**	6.4	81	72.7	147.6
BJ2	5	7	**–39.7**	**171.5**	9.8	49	81.6	–173.2
AU9	8	8	39.5	338.4	7.5	55	69.7	–182.9
AU10	7	8	40.4	340.5	8.9	40	71.6	–180.5
AU12	6	8	47.1	337.5	8.3	46	67.8	–167.4
AU14	5	6	48.6	324.9	11.1	26	56.8	–170.2
AU13	8	8	42.4	331.5	7.9	49	63.2	–178.8
AU15	7	8	32.6	332.7	8.4	45	64.1	–194.2
AU8	6	7	50.7	336.3	7.5	63	65.7	–160.9
AU1	8	8	50.5	329.4	8.3	45	60.2	–165.5
AU2	8	9	49.1	311.7	9.2	37	45.3	–171.3
AU3	8	8	43.3	343.2	5.1	122	73.5	–171.7
AU7	8	8	49.1	346.1	6.8	119	73.7	–152.4
AU5	6	8	**–27.3**	**152.5**	7.7	76	63.3	158.7
AU4	8	8	**–33.3**	**122.3**	6.5	93	35.7	–185.7
AU6	3	*3*	*55.9*	*321.8*	*21.4*	*8*	52.7	–159.6

As previously detected (*Goguitchaichvili et al., 2003*), the lowermost flows in the sequence yield reverse polarity magnetization (Table 1), and probably formed during chron 31r of the reference geomagnetic polarity time scale. The remaining flows, including those belonging to the radiometrically dated site, would correspond to chron 30n. However, if we consider the available age information, we cannot exclude that it possibly corresponds to chron 29r. Indeed, the age of the Autlan lava flows is 67.4 ± 1.2 Ma. If we consider the lower age, i.e. 66.2 Ma, it corresponds to the chron 29r of the Deccan traps from the Western Ghats in India recently dated by U-Pb methods on zircon (*Schoene et al., 2015*).

The average flow paleodirections are in general well determined (Table 1; Figs 4 and 5). No *ChRM* directions were isolated for site BJ06 (Table 1) because of erratic and noisy behavior during the both alternating field and thermal demagnetization. Almost all α_{95} values of the remaining 11 sites are less than 10°, except the unit BJ4, yielding α_{95} of 11.6° and the smaller value of the precision parameter k (42).

The mean paleodirection of the region (Table 2) was determined incorporating coeval, previous data from the same area as well (14 paleodirections reported in *Goguitchaichvili et al., 2003*, Table 1). Figures 4 and 5 illustrate all the site-mean directions and their corresponding Virtual Geomagnetic Poles (VGPs), together with the respective mean paleodirections and paleopoles. Note that the paleopole obtained in this study is statistically indistinguishable from that of *Goguitchaichvili et al. (2003)* (BJ and AU, respectively, in Table 2 and Fig. 5).

As there are only 4 site-mean directions of reversed polarity (vs. 19 of normal polarity), we cannot perform a reversal test with the assumption of a common Fisherian precision in both distributions (a poor-quality, positive test –indeterminate following the *McFadden and McElhinny (1990)* classification- is obtained using a simulation test without this assumption). Nevertheless, inclinations of the sites with reversed polarity data are lower than those observed in the normal polarity dataset (Table 1, Fig. 4).

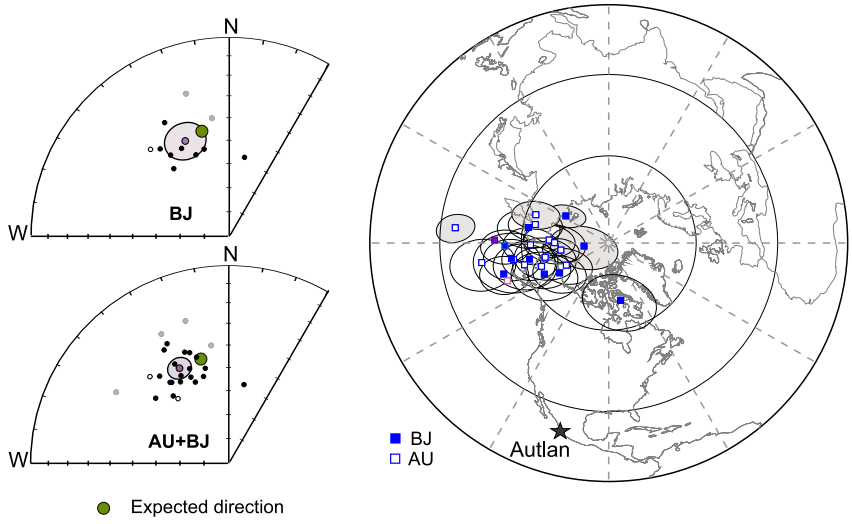

Fig. 4. **Left:** Equal area projections of the site-mean characteristic paleodirections for the Autlan volcanics (Top: this study, BJ samples; Bottom: all available data - AU+BJ samples). Grey circles indicate antipodal reversed polarities; blank circles directions from sites with $n < 5$. Mean directions of all sites in each dataset, surrounded by 95% confidence cones, are compared with the reference direction expected from coeval, selected North American paleomagnetic poles (see text and Fig. 5). **Right:** Equal area plot of Virtual Geomagnetic Poles (VGPs) for each individual, available flow, all projected in the northern hemisphere (after transformation of the reversed component to the northern hemisphere), with their 95% confidence ellipses (along the paleomeridian and perpendicular to it; around those VGPs from sites with $n > 5$), which are shaded when reversed polarities were observed.

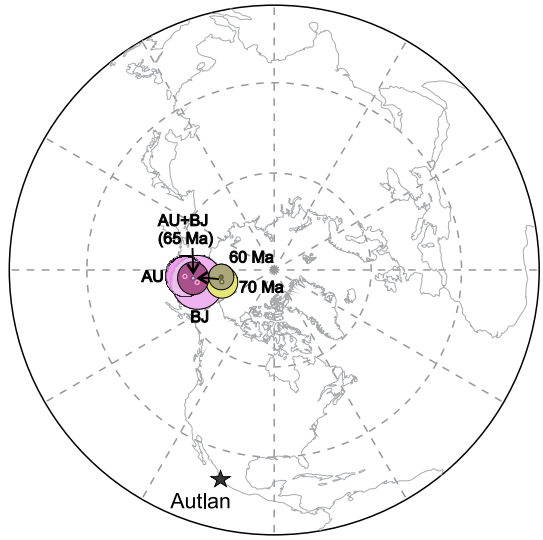

Fig. 5. Paleomagnetic poles obtained in this study (BJ samples), previously published (AU samples, *Goguitchaichvili et al., 2003*), and from the combined and selected dataset (AU+BJ samples), surrounded by 95% confidence cones, are anticlockwise, slightly (~10°) deviated from available 70 and 60 Ma reference poles (plotted those from *Torsvik et al., 2012*; for the North American Apparent Polar Wander Path).

A more selective dataset is also analyzed ($N = 23$, Table 2), satisfying both tectonic and PSV quality criteria with number of specimens $n > 5$ and $\alpha_{95} < 10°$ (with only two rejected sites: BJ4 and AU6). The mean directions of both datasets (number of sites $N = 25$ and 23, with all site-mean directions referred to the northern hemisphere) have similar α_{95} values and differ only in 1° (Table 2); being the mean paleodirection of the 23 selected sites: inclination $Inc = 44.7°$, declination $Dec = 333.6°$, $\alpha_{95} = 4.9°$. They are

Table 2. Summary of palaeomagnetic results of the different analysed data sets (selected: sites with $n > 5$). *N*: number of sites; *Dec*, *Inc*: mean directions (declination, inclination); *PLat, PLong*: corresponding mean pole latitude and longitude; *k*, α_{95}: precision parameter and semi-angle of 95% confidence for directional *(Fisher, 1953)*; *K*, A_{95}: the same for the pole space. BJ: this study; AU: *Goguitchaichvili et al. (2003).*

Data Set	*N*	*Dec* [°]	*Inc* [°]	*k*	α_{95} [°]	*PLat* [°]	*PLong* [°]	*K*	A_{95} [°]
BJ (all)	11	335.1	46.1	33	8.1	65.95	37.93	27	8.9
BJ selected	10	337.0	46.5	33	8.5	67.49	39.82	28	9.3
AU (all)	14	330.7	44.2	45	6.0	62.34	32.9	42	6.2
AU selected	13	331.2	43.3	46	6.1	62.87	31.49	42	6.5
AU+BJ (all)	25	332.6	45.0	40	4.6	63.94	34.83	35	5.0
AU+BJ selected	23	333.6	44.7	40	4.9	64.86	34.63	35	5.2

compared with the expected directions in the studied area (Fig. 4), as derived from available reference poles (*Besse and Courtillot, 2002*; *Kent and Irving, 2010*; *Torsvik et al., 2012*) for the North American craton, centered in 70 Ma and 60 Ma (Fig. 5). These reference poles come exclusively from North American poles (*Kent and Irving, 2010*) or also from globally distributed poles rotated to a North American frame (*Besse and Courtillot, 2002*; *Torsvik et al., 2012*); and their corresponding A_{95} values range from 2.1° to 5.5°. The precise dating age of the Autlan sequence, if older than previously reported, is not critical for the amount of the observed tectonic rotation, as the 70–100 Ma time window correspond with a steady segment of the Apparent Polar Wander Path (APWP) for North America (i.e., has similar reference paleopoles).

The same qualitative results are obtained, for the 70–60 Ma time window with these different reference poles, calculating the amounts of vertical-axis rotation R (observed minus expected declinations) and flattening of inclination F (expected minus observed inclinations), which have been evaluated with their confidence limits (ΔR and ΔF, *Demarest, 1983*): $R = -13° \pm 6°$ and $F = 2° \pm 5°$ (*Besse and Courtillot, 2002*); or $R = -14° \pm 7°$ and $F = 0° \pm 7°$ (*Kent and Irving, 2010*); or $R = -10° \pm 6°$ and $F = -1° \pm 5°$ (*Torsvik et al., 2012*; GAPWP in North American frame); or $R = -11° \pm 7°$ and $F = -1° \pm 6°$ (*Torsvik et al., 2012*; North American APWP, Fig. 5). All F values, indicate that the observed mean inclination is always in a very good agreement with the expected inclinations. The observed declination, however, is always significantly ($\Delta R < |R|$) different from those expected ones, which suggests a relatively small, counterclockwise (ranging from $-10° \pm 6°$ to $-14° \pm 7°$) vertical-axis tectonic rotation (Figs 4 and 5) in the Autlan sequence.

Regarding PSV, the classical formula $S_B^2 = S_T^2 - S_W^2 / n$ (e.g., *McFadden et al., 1991*) was used for estimating the angular dispersion of VGPs in this study. Here, S_T is total angular dispersion (*Cox, 1970*)

$$S_T = \left[\frac{1}{N-1} \sum_{i=1}^{N} \delta i^2 \right]^{1/2},$$

where N is number of sites used in calculation, δi the angular distance of the i-th VGP from the mean paleomagnetic pole. S_W represents the within site dispersion (n being the average number of samples per unit), and in this study it has been evaluated following *McElhinny and McFadden (1997)*, where it is determined from the latitude λ and the arithmetic average of the α_{95} per lava flow (α_{95avg} in Table 3).

Using the iterative process defined by *Vandamme (1994)* to obtain optimum, latitudinal variable cut-off angles Θ (which directly depend on the angular dispersion of each VGP data set distribution as $\Theta = 1.8 S_T + 5°$), we obtained a geomagnetic dispersion value (Table 3, Fig. 6) of $S_B = 9.6°$ (upper and lower limits: 7.2° and −11.9° if bootstrapped or 7.9° and −12.1° using those from *Cox, 1969*) for the selected dataset (starting with $N = 23$), in perfect agreement (Fig. 6) with the compilation of selected Cretaceous data from lavas reported in *Biggin et al. (2008)*. These values barely change if all data (starting with $N = 25$) are analyzed (Table 3).

Table 3: Ultimate iteration of paleosecular variation results of the *Vandamme (1994)* iterative method. N: number of non-excluded virtual geomagnetic poles (VGP); N_T: number of total VGPs; α_{95avg}: average semi-angle of 95% confidence; D_{max}: maximum angle from the mean; Θ: *Vandamme (1994)* optimum cut-off angle ($1.8\,S_T + 5°$); S_T: total angular dispersion; S_B: geomagnetic field dispersion. S_L and S_U: lower and upper 95% bootstrapped confidence limits of S_B.

Data set	N	N_T	α_{95avg} [°]	D_{max} [°]	Θ [°]	S_T [°]	S_B [°]	S_L [°]	S_U [°]
All	23	25	10.1	18.7	24.7	10.9	9.4	6.9	11.3
Selected ($n > 5$)	21	23	8.1	19.8	24.0	10.6	9.6	7.2	11.9

Alternatively, using a fixed cut-off angle of 45° (e.g., *Johnson et al., 2008*), identical results are obtained in both datasets: The maximum angle from the mean of all VGPs is 33° (<45°), and a geomagnetic dispersion value of $S_B = 12.2°$ is obtained. This compare favorably with *McFadden et al. (1991)* results, who using also a 45° cutoff angle, report on a VGP scatter centered around 11.5°, for the ±20° latitude band, from their compilation of lavas dated between 45 and 80 Ma.

Despite the reversed polarity mode is only represented in a 16% of the data, it seems that its associated geomagnetic dispersion is slightly higher than that of the normal polarity mode (e.g., *McElhinny and McFadden, 1997*). Reversed directions have lower inclinations and corresponding VGPs are farthest from Autlan location (Fig. 4), thus with greater angular distances from the mean paleopole (Fig. 5).

Absolute paleointensity experiments performed in this study failed completely probably due to the presence of dominantly multidomain magnetic grains. Only acceptable results from this region (lva flows of same sequence) belongs to study reported by *Goguitchaishvili et al. (2004)*. The mean VDM obtained for Autlan lavas (Fig. 7) is about 63% of the present geomagnetic axial dipole (7.8×10^{22} Am^2 after *Barton et al., 1996*) but in reasonably good agreement with other comparable quality determinations between 5 and 90 Ma.

The relationship between reversal rate and absolute intensity is still matter of debate. *Aubert et al., (2010)* performed numerical geodynamo predictions and analyzed available (selected) paleomagnetic data including absolute intensities for the last 200 Ma. This analysis indicates that an inverse relationship exists between the geomagnetic field strength and reversal rates. In the same context, *Tarduno and Cottrell (2005)* carried out a comprehensive absolute intensity study of plagioclase crystals to examine distinct characteristic geodynamo regimes over the geological periods (period of moderate reversal frequency, practically non-reversing field of the Cretaceous Normal Polarity Superchron and a period of high reversal occurrence during the Jurassic). Again, a well-marked inverse relationship between reversal rate and intensity is observed. In addition, the authors argued that the geomagnetic field strength of reversing field is more variable than that of the non-reversing field. Thus, our paleointensity data contradicts with observed relationship between intensity and reversal rate. As already mentioned by *Tarduno and Smirnov (2004)* there are many natural and experimental routes that lead to

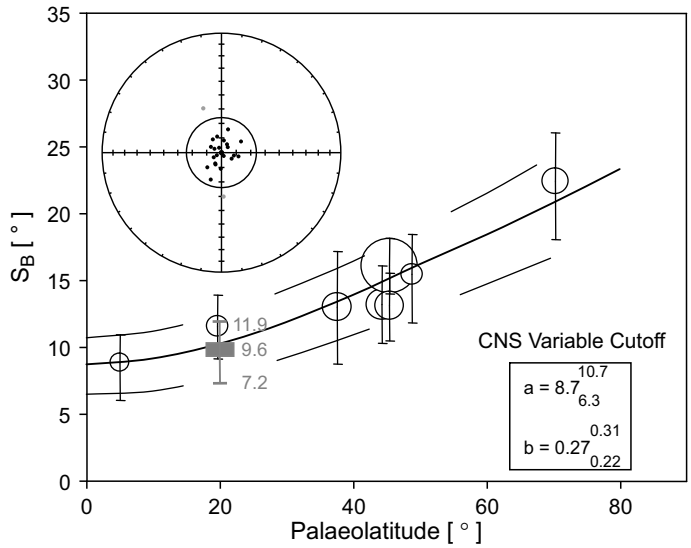

Fig. 6. Autlan virtual geomagnetic poles (VGP) dispersion ($S_B = 9.6°$, filled rectangle) with its 95% bootstrap uncertainty limits, is integrated in the VGP dispersion curve (VGP scatter against geographic latitude) of *Biggin et al. (2008)* for the Cretaceous Normal Superchron (CNS), where open circles refer to other results from lavas at different paleolatitudes after applying variable cut-offs (*Vandamme, 1994*) to high-quality CNS datasets. (Bottom inset): The shape parameters (a, b) of the best-fit Model G (*McFadden et al., 1988*) with 95% bootstrap uncertainty limits are given in an inset, and the resulting curves plotted. ('Model G' described VGP dispersion in terms of symmetric and anti-symmetric contributions; the former is constant and the latter dependent of latitude λ: $S_B = \sqrt{a^2\lambda^2 + b^2}$. Upper inset: Equal area projection of considered 23 VGPs centred on their mean direction (unspecified longitudes), showing the effect of the *Vandamme (1994)* variable cut-off angle (two rejected sites outside the circle).

alteration of lava samples that are typically used in paleointensity experiments. Presence of multidomain grains, maghemitization due to the hydrothermalism and potential adquisition of thermochemical remanent magnetization during the laboratory heatings may overestimate the absolute paleointensity values.

Concerning the long-term evolution of the geomagnetic field strength we note that three main tendencies may be observed judging from existing available data-set. The data based on natural rocks (mainly basaltic lava flows) suggests the low paleointensity during whole Mesozoic time ('Mesozoic Dipole Low', first underlined by *Prévot et al., 1990*). Submarine basaltic glass data supports the relatively high paleointensity since about present with lower paleointensities prior to that including whole CNS. In contrast, *Tarduno et al. (2001, 2002)* suggest that the paleointensity was higher during CNS. Thus the interpretation depends on material used.

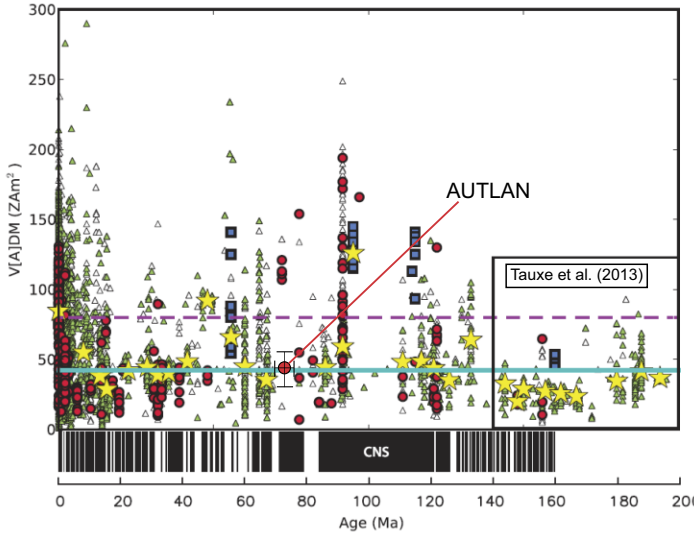

Fig. 7. Recent compilation of available absolute paleointensity data in terms of virtual dipole moments. (*Tauxe et al., 2013*, © American Geophysical Union).

5. CONCLUSIONS

The Autlan volcanic succesion is revisited adding new entries to conform a robust database around 65–70 Ma within the Jalisco block, western Mexico. Tentative magnetostratigraphic correlations, with reversed polarities found at the base of the sequence and normal polarities above, suggest that the entire volcanic sequence was emplaced during a time span of about 2 Ma prior to the K-T limit.

The obtained paleodirections are statistically useful for tectonic and geomagnetic purposes, with observed inclinations matching the expected ones but with observed declinations westerly deviated from the expected ones, as inferred from available 60–70 Ma reference poles for stable North America (*Besse and Courtillot, 2002*; *Kent and Irving, 2010*; *Torsvik et al., 2012*).

The apparent counterclockwise vertical-axis rotation affecting Autlan volcanics ($|R| \sim 10^{\circ} - 14^{\circ}$) is statistically significant ($\Delta R \sim 6°–7°$), and do not depend of the choice of the reference paleopoles (and therefore independent of their source: North American poles only or globally distributed poles in the North American frame by a selected plate circuit). We should emphasize however, that original flow plane is hard to retrieve in the field, and therefore we cannot provide strong information about tectonic rotation. As already mentioned, there are no sedimentary layers intercalated within Autlan lava flow sequences and thus the bedding plane orientation measured in the field is considered as original plane. If this assumption was erroneous, then all discusion about observed tectonic rotation may be compromised.

PSV from Autlan volcanics, determined from its geomagnetic dispersion (e.g., S_B value of 9.6° - from 7.2° to 11.9° - calculated using a variable VGP cutoff), agree with previous selected PSV (paleosecular variation) results from compilations of lavas of coeval age (*McFadden et al., 1991*; *Biggin et al., 2008*). In addition, it reinforces the significance of the tectonic rotation indicating that PSV has been adequately averaged.

This study evidence the difficulties to obtain absolute paleointensity determination form the volcanic rocks older than 5 Ma since less than 5% success rate are achieved. The mean VDM (virtual dipole moement) obtained for Autlan lavas reinforces the hypothesis (*Tauxe et al., 2013*) of low geomagnetic field strengths extending into the Upper Cretaceous.

Acknowledgments: The financial support was given by UNAM-PAPIIT project IA102213 and CONACyT Ciencia Basica (CB-2009-01—00131191). VCRM thanks to the CGL (2011-29474-C02-01) DGI I+D+i Spanish project. AG acknowledges the partial support from UNAM-DGAPA-PAPIIT project IN10524.

References

Barton C.E., Baldwin R., Barraclough D., Bushati S., Chiappini M., Cohen Y., Coleman R., Hulot G., Kotze V., Golovkov V., Jackson A., Langel R., Lowes F., McKnight D., Macsmillan S., Newitt L., Peddie N., Quinn J. and Sabaka T., 1996. International geomagnetic reference field, 1995 revision. *Geophys. J. Int.*, **125**, 318–321.

Besse J. and Courtillot V., 2002. Apparent and true polar wander and the geometry of the geomagnetic field over the last 200 Myr. *J. Geophys. Res.*, **107(B11)**, DOI: 1029 /2000JB000050.

Biggin A.J., Van Hinsbergen D.J., Langerais C.G., Straathof G.B. and Deenen M.H.L., 2008. Geomagnetic secular variation in the Cretaceous Normal Superchron and in the Jurassic. *Phys. Earth Planet. Inter.*, **169**, 3–19, DOI: 10.1016/j.pepi.2008.07.004.

Böhnel H., Alva-Valdivia L., Gonzalez-Huesca S., Urrutia-Fucugauchi J., Moran-Zenteno D.J. and Schaaf P., 1989. Paleomagnetic data and the accretion of the Guerrero Terrane, Southern Mexico Continental Margin. In: Hillhouse J.W. (Ed.), *Deep Structure and Past Kinematics of Accreted Terranes*. American Geophysical Union, Washington, D.C., 73–92, DOI: 10.1029 /GM050p0073

Campa U.M.F. and Coney P., 1983. Tectonostratigraphic terranes and mineral resource distribution in Mexico. *Can. J. Earth Sci.*, **20**, 1040–1051.

Coe R., 1967. Paleointensity of the Earth's magnetic field determined from Tertiary and Quaternary rocks. *J. Geophys. Res.*, **83**, 1740–1756.

Cox A., 1969. Research note: Confidence limits for the precision parameter, K. *Geophys. J. R. Astr. Soc.*, **17**, 545–549.

Cox A., 1970. Latitude dependence of the angular dispersion of the geomagnetic field. *Geophys. J. R. Astr. Soc.*, **20**, 253–269.

Day R., Fuller M.D. and Schmidt V.A., 1977. Hysteresis properties of titanomagnetites: grain size and composition dependence. *Phys. Earth Planet. Inter.*, **13**, 260–267.

Demarest H.H., 1983. Error analysis for the determination of tectonic rotation from paleomagnetic data. *J. Geophys. Res.*, **88**, 4321–4328.

Dunlop D.J., 2002. Theory and application of the Day plot (Mrs/Ms versus Hcr/Hc) 1. Theoretical curves and tests using titanomagnetite data. *J. Geophys. Res.*, **107(B3)**, 2056.

Fisher R.A., 1953. Dispersion on a sphere. *Proc. R. Soc. London A*, **217**, 295–305.

Goguitchaitchvili A. 2011. A comprehensive rockmagnetic, paleomagnetic, paleointensity and geochronologic study along the western Trans-Mexican Volcanic Belt: geodynamic and geomagnetic implications. *Geofis. Int.*, **502**, 227–254.

Goguitchaichvili A., Alva-Valdivia L.M., Rosas-Elguera J., Urrutia-Fucugauchi J. and Solé J., 2004. Absolute geomagnetic paleointensity after the Cretaceous Normal Superchron and just prior to the Cretaceous-Tertiary transition. *J. Geophys. Res.*, **109**, B01105, DOI: 10.1029 /2003JB002477.

Goguitchaichvili A., Alva-Valdivia L.M., Urrutia-Fucugauchi J. and Rosas-Elguera J., 2003. A combined paleomagnetic and geochronology study of Late Cretaceous volcanic sequence in Western Mexico. *Int. Geol. Rev.*, **45**, 886–897.

Goguitchaitchvili A., Alva-Valdivia L.M., Urrutia-Fucugauchi J. and Morales J., 2002. On the reliability of Mesozoic dipole low: New absolute paleointensity results from Parana flood basalts (Brazil). *Geophys. Res. Lett*., **29**, 1655, DOI: 10.1029/2002GL015242.

Grommé C.S., Wright T.L. and Peck D.L., 1969. Magnetic properties and oxidation of iron-titanium oxide minerals in Alae and Makaopuhi lava lakes, Hawaii. *J. Geophys. Res.*, **74**, 5277–5294.

Kent D.V. and Irving E., 2010. Influence of inclination error in sedimentary rocks on the Triassic and Jurassic apparent pole wander path for North America and implications for Cordilleran tectonics. *J. Geophys. Res.*, **115**, B10103.

Kirschvink J.L., 1980. The least-squares line and plane and the analysis of palaeomagnetic data. *Geophys. J. R. Astr. Soc.*, **62**, 699–718.

Leonhardt R., 2006. Analyzing rock magnetic measurements: The rockmaganalyzer 1.0 software. *Comput. Geosci.*, **32**, 1420–1431.

McElhinny M.W. and McFadden P.L., 1997. Palaeosecular variation over the past 5 Myr based on a new generalized database. *Geophys. J. Int*., **131**, 240–252.

McFadden P.L. and McElhinny M.W., 1990. Classification of the reversal test in palaeomagnetism. *Geophys. J. Int*., **103**, 725–729.

McFadden P.L., Merrill R.T. and McElhinny M.W., 1988. Dipole quadrupole family modelling of paleosecular variation. *J. Geophys. Res*., **93**, 11583–11588, DOI: 10.1029/JB093iB10p11583.

McFadden P.L., Merrill R., McEllhinny M.W. and Lee S., 1991. Reversals of the Earth's magnetic field and temporal variations of the dynamo families. *J. Geophys. Res*., **96**, 3923–3933.

Ortega-Gutiérrez F., Elías-Herrera M., Morán-Zenteno D.J., Solari L., Luna-González L. and Schaaf P., 2014. A review of batholiths and other plutonic intrusions of Mexico. *Gondwana Res.*, **26**, 834–868.

Perrin M. and Shcherbakov V.P., 1997. Paleointensity of the Earth magnetic field for the past 400 My: Evidence for a dipole structure during the Mesozoic low. *J. Geomag. Geoelectr.*, **49**, 601–614.

Prevot M., Derder M.E.M., McWilliams M. and Thompson J., 1990. Intensity of the Earth's magnetic field: Evidence for a Mesozoic dipole low. *Earth Planet. Sci. Lett*., **97**, 129–139.

Rosas-Elguera J., Ferrari L., Martinez M. and Urrutia-Fucugauchi J., 1997. Stratigraphy and tectonics of the Guadalajara region and triple-junction area, western Mexico. *Int. Geol. Rev*., **39**, 125–140.

Ruiz-Martínez V.C., Urrutia-Fucugauchi J. and Osete M.L., 2010. Palaeomagnetism of the Western and Central sectors of the Trans-Mexican volcanic belt: implications for tectonic rotations and palaeosecular variation in the past 11 Ma. *Geophys. J. Int.*, **180**, 577–595, DOI: 10.1111 /j.1365-246X.2009.04447.x.

Shoene B., Samperton K.M., Eddy M., Keller G., Adatte T., Bowring S., Khadri S. and Gartsh B., 2015. U-Pb geochronology of the Deccan Traps and relation to the end-Cretaceous mass extinction. *Science*, **347**, 6218, 182–185.

Tanaka H., Kono M. and Uchimura H., 1995. Some global features of paleointensity in geological time. *Geophys. J. Int.*, **120**, 97–102.

Tarduno J.A. and Cottrell R.D., 2005. Dipole strength and variation of the time-averaged reversing and nonreversing geodynamo based on Thellier analyses of single plagioclase crystals. *J. Geophys. Res.*, **110**, B11101, DOI: 10.1029JB 003970.

Tarduno J.A. and Smirnov A.V., 2004. The paradox of low field values and the long-term history of the geodynamo. In: Channell J.E.T., Kent D.V., Lowrie W. and Meert J.G. (Eds), *Timescales of the Paleomagnetic Field*. American Geophysical Union, Washington, D.C., 75–84, DOI: 10.1029/145GM06.

Tarduno J.A., Cottrell R.D. and Smirnov A.V., 2001. High geomagnetic intensity during the Mid Cretaceous from Thellier analyses of single plagioclase crystals. *Science*, **291**, 1779–1783.

Tarduno J.A., Cottrel R.D. and Smirnov A.V., 2002. The Cretaceous superchron geodynamo: Observations near the tangent cylinder. *Proc. Natl. Acad. Sci. U. S. A.*, **99**, 14020–14025, DOI: 10.1073/pnas.222373499.

Tauxe L. and Staudigel H., 2004. Strength of the geomagnetic field in the Cretaceous Normal Superchron: New data from submarine basaltic glass of the Troodos Ophiolite. *Geochem. Geophys. Geosyst.*, **5**, Q02H06, DOI: 10.1029/2003GC000635.

Tauxe L., Gee J.S., Steiner M.B. and Staudigel H., 2013. Paleointensity results from the Jurassic: New constraints from submarine basaltic glasses of ODP Site 801C. *Geochem. Geophys. Geosyst.*, **14**, 4718–4733, DOI: 10.1002/ggge.20282.

Thellier E. and Thellier O., 1959. Sur l'intensité du champ magnétique terrestre dans le passé historique et géologique. *Ann. Géophys.*, **15**, 285–376 (in French).

Torsvik T.H., Van der Voo R., Preeden U., Mac Niocaill C., Steinberger B., Doubrovine P.V., van Hinsbergen D.J.J., Domeier M., Gaina C., Tohver E., Meert J.G., McCausland P.J.A. and Cocks L.R.M., 2012. Phanerozoic polar wander, palaeogeography and dynamics. *Earth Sci. Rev.*, **114**, 325–368.

Valencia V., Righter K., Rosas-Elguera J., Lopez-Martínez M. and Grove M., 2013. The age and composition of the pre-Cenozoic basement of the Jalisco Block: implications for and relation to the Guerrero composite terrane. *Contrib. Mineral. Petrol.*, **166**, 801–824.

Vandamme D.A., 1994. A new method to determine paleosecular variation. *Phys. Earth Planet. Inter.*, **85**, 131–142, DOI: 10.1016/0031-9201(94)90012-4.

Wallace P., Carmichael I.S.E., Righter K. and Becker T., 1992. Volcanism and tectonism in western Mexico: A contrast of style and substance. *Geology*, **20**, 625–628.